Stratospheric–Tropospheric Mass Exchange during the Presidents' Day Storm

PAUL SPAETE

Space Science and Engineering Center, University of Wisconsin—Madison, Madison, Wisconsin

DONALD R. JOHNSON

Space Science and Engineering Center and Department of Atmospheric and Oceanic Sciences, University of Wisconsin—Madison, Madison, Wisconsin

TODD K. SCHAACK

Space Science and Engineering Center, University of Wisconsin—Madison, Madison, Wisconsin

(Manuscript received 23 February 1993, in final form 10 September 1993)

ABSTRACT

Using data generated from a model simulation, the exchange of mass between the stratosphere and the troposphere is estimated for the Presidents' Day storm during a 24-h period beginning at 1500 UTC 18 February 1979. This 24-h interval coincided with a strongly developed tropopause depression and the onset of explosive surface cyclogenesis. The initial part of the study consists of identifying a surface of isentropic potential vorticity (IPV) to represent the tropopause. The 3.0-IPV-unit surface is chosen since the pressure distribution on this surface closely matches the tropopause pressures reported by radiosonde stations. The IPV surface portrays the depression of the tropopause associated with the polar-front jet and trough system accompanying the baroclinic amplification of the Presidents' Day storm.

Using a quasi-Lagrangian transport model, stratospheric–tropospheric mass exchange is estimated for the region including and immediately adjacent to the tropopause depression. The estimated mass transport from the stratosphere to the troposphere for the 24-h period is 5×10^{14} kg. The transport from the troposphere to the stratosphere is 2×10^{14} kg yielding a net transport across the tropopause of 3×10^{14} kg from the stratosphere to the troposphere. These results are confirmed by a second, independent model simulation.

The mass transport from stratosphere to troposphere across the 3.0-IPV surface coincides with descending air, often referred to as the "dry airstream," arcing counterclockwise around the polar-front jet and trough system from northwest to east. Reverse transport from the troposphere to the stratosphere occurs northeast of the depression and agrees with trajectories of air parcels within the end region of rising "conveyer belts."

1. Introduction

The intense cyclone development along the mid-Atlantic coast on 18–19 February 1979, known as the Presidents' Day storm, was accompanied by a pronounced depression of the tropopause (Uccellini et al. 1985). The depression occurred in conjunction with an eastward-propagating polar-front jet stream and trough. These systems and the accompanying tropopause depressions have been identified as important centers of exchange between the stratosphere and troposphere (Staley 1962; Reiter 1975). Despite the recognized importance of these systems, only a few quantitative exchange estimates exist in the literature (e.g., Reiter and Mahlman 1965; Reiter et al. 1969).

The synoptic and dynamical aspects of the Presidents' Day storm have been extensively studied by numerous investigators (e.g., Bosart 1981; Bosart and Lin 1984; Uccellini et al. 1984, 1985). Additionally, numerical simulations of the storm have been conducted in order to more precisely identify processes occurring during development (e.g., Atlas 1987; Uccellini et al. 1987; Whitaker et al. 1988).

Using simulated data from the Mesoscale Analysis and Simulation System (MASS) numerical model discussed in Whitaker et al. (1988), the present study first identifies the tropopause using an isentropic potential vorticity (IPV) criterion and then estimates the mass exchange between the stratosphere and the troposphere across this surface. Transport is investigated using the diagnostic model of Wei (1987) applied within a quasi-Lagrangian reference system. Wei's diagnostic model

Corresponding author address: Dr. Paul Spaete, Space Science and Engineering Center, University of Wisconsin—Madison, Madison, WI 53706.

has been used previously by Hoerling et al. (1993) to estimate global transport. The present study represents an initial attempt to apply the diagnostic model to a moving system of limited scale. Emphasis will be placed on the determination of an appropriate value of IPV for defining the tropopause and on the estimation of the stratospheric–tropospheric mass exchange associated with the storm.

A description of the methodology is presented in section 2. Section 3 contains a description of the numerically simulated storm. The procedure for determining the tropopause surface is discussed in section 4. Attention is given to specifying an IPV surface on which the correlation between the IPV-determined tropopause pressures and the radiosonde-reported tropopause pressures is maximized within the model domain. Section 5 will discuss the mass exchange between the stratosphere and troposphere using Wei's diagnostic model applied within a quasi-Lagrangian reference system moving with the tropopause depression accompanying the rapidly propagating polar jet (PJ)–trough system. The results of the study are summarized in section 6.

2. Methodology

Uccellini et al. (1987) and Whitaker et al. (1988) employed the MASS numerical model for studies of the Presidents' Day storm. The model grid consisted of 32 equally spaced sigma levels bounded vertically by the earth's surface and 100 mb within a 128 × 96 horizontal gridpoint array having a constant separation of 58.5 km. The present study is based on the Whitaker et al. (1988) simulation, which was able to successfully depict the evolution of the tropopause depression and surface system.

For this study, the model-simulated data had been interpolated vertically to 38 isentropic levels with 4-K vertical resolution from 248 to 396 K. Horizontally, the model results had been interpolated to a 0.5° latitude–longitude grid with 43 rows and 85 columns, bounded on the north and west by 50.0°N and 107°W. Additional processing of the data was completed at the University of Wisconsin to produce a consistent isentropic dataset extending down to 220 K.

Wei (1987) developed a diagnostic model in which transport across the tropopause is regarded conceptually as transport across a parametric boundary (Johnson 1977). Wei's transport model is designed to work with any continuous surface representing the boundary between the stratosphere and troposphere. In this study, isentropic potential vorticity will be used to define the tropopause surface, and field quantities will be interpolated to this surface from isentropic coordinates. The estimate of mass transport across the tropopause in this study uses a modification of Wei's diagnostic model appropriate for a quasi-Lagrangian reference system moving horizontally with the tropopause depression (Johnson and Downey 1975). In this quasi-Lagrangian system, the mass transport through the tropopause is expressed as

$$F(\rho) = \rho J_\theta \left[\frac{d\theta}{dt} - \frac{\delta\theta}{\delta t_{Q_0}} - (\mathbf{U} - \mathbf{W}) \cdot \nabla_{Q_0} \theta \right], \quad (1)$$

where Q_0 represents the tropopause surface, $\rho J_\theta = -g^{-1} \partial p / \partial \theta$ is the hydrostatic isentropic mass density, $\mathbf{W}$ is the horizontal velocity of the point of highest pressure on the IPV surface defining the tropopause depression, and $\delta\theta/\delta t_{Q_0}$ is the quasi-Lagrangian tendency of potential temperature on the tropopause surface.

As discussed in Wei (1987) and Hoerling et al. (1993), the mass transport through the tropopause is determined as the sum of three processes on the right-hand side of (1). From left to right, these processes involve 1) diabatic heating, 2) the quasi-Lagrangian tendency of tropopause potential temperature, and 3) the quasi-Lagrangian advection of potential temperature along the tropopause. The evaluation of (1) requires specification of zonal wind u, meridional wind v, potential temperature θ, mass ρJ_θ, and diabatic mass flux $\rho J\dot{\theta}$, on the tropopause surface. The diabatic mass flux is first computed on isentropic levels through vertical integration of the isentropic mass continuity equation as discussed in Schaack et al. (1990). The diabatic mass flux and other parameters are interpolated from isentropic surfaces to the IPV-defined tropopause assuming a linear variation with p^κ ($\kappa = R/C_p$).

Processes corresponding to those on the right-hand side of (1) would also be present in an Eulerian system. Formulating the transport computations within a quasi-Lagrangian system may seem to add an unnecessary degree of complexity. However, the purpose of this study is to isolate the relative transport associated with the moving PJ–trough system. The most practical way to accomplish this is to use a computational domain moving with the tropopause depression. Additionally, quasi-Lagrangian calculations are more consistent with the many studies of airstreams associated with extratropical cyclones (e.g., Carlson 1980; Kuo et al. 1992).

The transport estimates derived from (1) are based on the implicit assumption that stratospheric and tropospheric air parcels crossing the tropopause are incorporated into the tropospheric and stratospheric portions of the atmosphere, respectively. With this assumption, estimates derived from (1), which are based on time scales of a day and evaluated over limited areas, represent upper bounds for actual exchange.

The IPV is computed according to

$$\text{IPV} = -g(f + \zeta_\theta)\left(\frac{\partial p}{\partial \theta}\right)^{-1}, \quad (2)$$

where ζ_θ is the relative vorticity on an isentropic surface and f is the Coriolis parameter. Wei's transport model requires that the surface used to represent the

tropopause must be a single-valued function of (x, y). To satisfy this condition, a vertical distribution of IPV surfaces is constructed as follows. When a given value of IPV occurs at multiple locations within a vertical column, the IPV surface is assigned to the location having the lowest pressure (highest elevation). With this procedure, a folded IPV surface is replaced by a steeply sloping surface on a discrete data grid according to the schematic in Fig. 1. The resulting IPV distribution within the upper troposphere and lower stratosphere becomes a monotonically increasing function of height; a redefinition that is analogous to the treatment of isentropic surfaces in the presence of superadiabatic layers. The tropopause is then represented by the IPV surface determined to best depict a boundary between the troposphere and stratosphere.

Another condition imposed in identifying the tropopause pressure is that the tropopause must occur at least 150 mb above the earth's surface. This precludes definition of a tropopause surface from high values of IPV associated with boundary-layer temperature inversions or from the strong cyclonic vorticity within the extratropical cyclone's low-level circulation.

Transport through an IPV surface implies sources and sinks of potential vorticity. Following Hoerling et al. (1993), with modifications for a quasi-Lagrangian system, the relationship between $F(\rho)$ and IPV sources and sinks is now discussed. The derivative of potential temperature in a quasi-Lagrangian system with coordinates (x, y, Q, t), where Q denotes a constant IPV surface, is given by

$$\frac{d\theta}{dt} = \frac{\delta\theta}{\delta t_Q} + (\mathbf{U} - \mathbf{W})\cdot\nabla_Q\theta + \dot{Q}\frac{\partial\theta}{\partial Q}. \qquad (3)$$

Multiplication of (3) by ρJ_θ and substitution into equation (1) yields

$$F(\rho) = \rho J_Q \dot{Q}, \qquad (4)$$

where $\dot{Q}$ represents "vertical motion" with respect to the IPV coordinate surface and $\rho J_Q = -g^{-1}\partial p/\partial Q$ is the hydrostatic mass density per incremental volume element $(\Delta x \Delta y \Delta Q)$ within the IPV coordinate framework discussed above. The preceding steps verify that the cross-tropopause transport $F(\rho)$ determined from (1) is equivalent to the mass transport due to IPV sources and sinks.

3. Model simulation of storm

The Presidents' Day storm is briefly discussed using analyses of Montgomery streamfunction and isotachs on the 312-K surface (Fig. 2) and cross-sectional analyses of potential temperature and IPV for selected times (Fig. 3). The bold dark lines on the 312-K analyses in Fig. 2 identify the locations of the cross sections. The feature of greatest importance in this discussion is the eastward propagation of the PJ–trough system and the accompanying high IPV values. A more detailed discussion of the mesoscale simulation, including surface analyses, is presented by Whitaker et al. (1988).

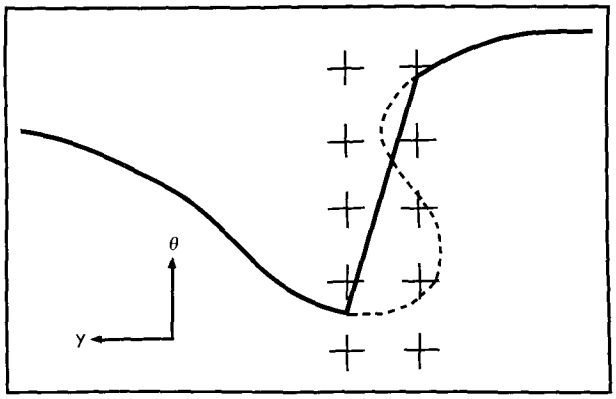

FIG. 1. Schematic illustrating the procedure used to redefine a folded IPV surface (dashed line) on a discrete grid. Solid line indicates the redefined surface, while vertical and horizontal grid points are denoted by crosses.

At 1200 UTC 18 February 1979, the initial time of the model simulation, a trough axis is located just west of the Mississippi River (Fig. 2a). An associated polar-front jet is centered over South Dakota and Nebraska with maximum wind speeds exceeding 40 m s^{-1} on the 312-K surface. The vertical cross section along the axis of the PJ–trough system at this time shows a potential vorticity maximum extending downward in the vicinity of an upper-tropospheric frontal zone (Fig. 3a). At the surface, an inverted trough is orientated along the Mississippi and Ohio River valleys (not shown).

By 0000 UTC 19 February (Fig. 2b), the polar-front jet is located near the base of the trough over western Kentucky. Maximum winds now exceed 50 m s^{-1} as the upper-tropospheric frontal zone strengthens, while the region of high IPV continues to display a downward extension in the vicinity of the frontal zone. A closed surface cyclonic circulation develops east of South Carolina in association with a coastal trough (not shown).

During the next 12 h, the PJ–trough system and associated values of high IPV propagate into the region of the East Coast extratropical cyclone. This coincides with the initiation of explosive surface development. During the remaining 12 h of the model simulation, between 1200 UTC 19 February and 0000 UTC 20 February, the trough on the 312-K surface propagates off the East Coast as explosive surface development continues.

In addition to the polar-front jet, a particularly intense subtropical jet occurs within the model domain during the first portion of the simulation (Fig. 2). Initially, the axis extends along the central Mississippi Valley, through the Ohio Valley, and over the Atlantic Ocean east of New York. Strong anticyclonic shear is present south of the axis. As the simulation progresses,

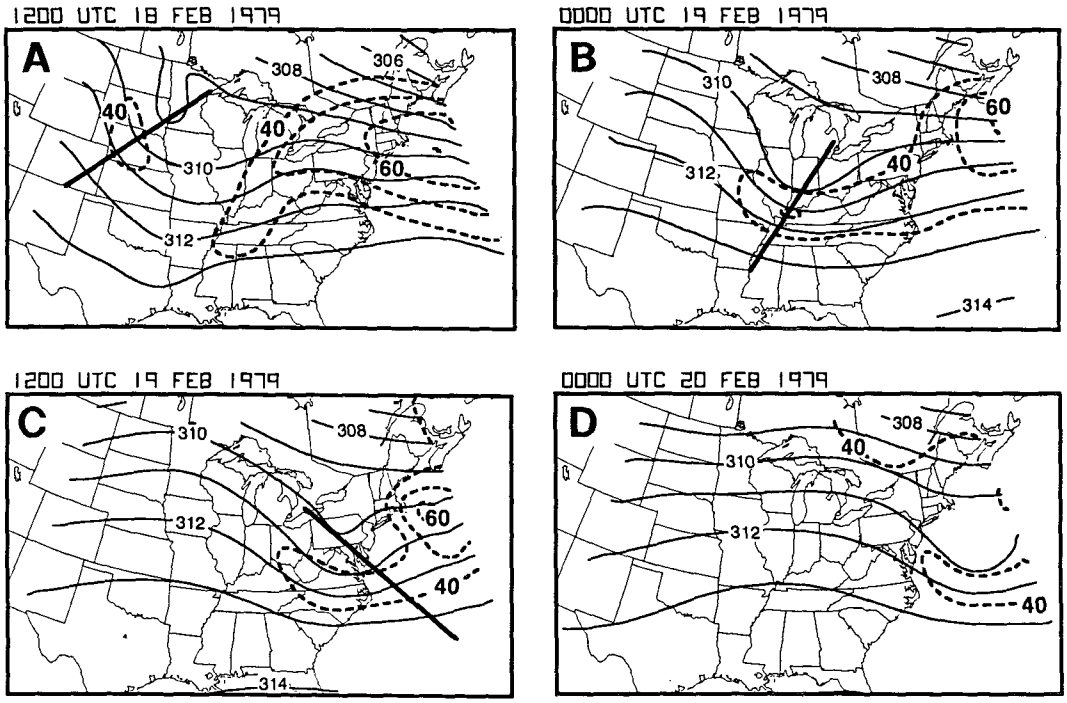

FIG. 2. Analyses of Montgomery streamfunction (10^3 m^2 s^{-2}) and isotachs (m s^{-1}) on the 312-K isentropic surface at (a) 1200 UTC 18 February, (b) 0000 UTC 19 February, (c) 1200 UTC 19 February, and (d) 0000 UTC 20 February 1979. Isotachs less than 40 m s^{-1} are not shown. Bold straight lines indicate the location of cross sections in Fig. 3.

the jet axis moves off the East Coast and the anticyclonic shear decreases over the model domain.

4. Determination of the tropopause surface

A uniquely defined boundary separating the stratosphere and troposphere is required to calculate exchange between the two regions. A traditional method for determining this boundary, still used in radiosonde station reports, is based on defining the tropopause through a specified lapse-rate discontinuity. However, such a criterion has been shown to produce ambiguities in the vicinity of jets and upper-level fronts (Reiter 1975).

Investigations have suggested that better spatial and temporal continuity is possible using a surface of constant IPV to define the tropopause (e.g., Reed 1955; Danielson and Hipskind 1980). However, the appropriate value of IPV is uncertain. This concern may be particularly important when using model results due in part to the effects of model resolution. The report on the Global Ozone Research and Monitoring Project (World Meteorological Organization 1986) suggested a value of 1.6×10^{-6} K m^2 kg^{-1} s^{-1} (subsequently referred to as 1.6 IPV units), which was inferred from time and zonally averaged cross sections of IPV and potential temperature. However, Hoerling et al. (1991) found that values between 3.0 and 4.0 IPV units yielded the most realistic tropopause pressure analysis for January 1979 using the European Centre for Medium-Range Weather Forecasts (ECMWF) global analyses. Considerable effort is now given to determining the value of IPV most appropriate for representing the tropopause.

As a first step, an assumption is made that tropopause pressures reported by radiosonde stations lying within the model domain provide the standard against which the pressures on IPV surfaces determined from the model data can be judged. The pressures on IPV surfaces at model grid points nearest the station locations are compared to the reported tropopause pressures at 1200 UTC 18 February, and 0000 and 1200 UTC 19 February for surfaces within the range of 1.5–4.0 IPV units. This interval encompasses the 1.6 IPV units suggested by the Global Ozone Research and Monitoring Project (World Meteorological Organization 1986) and the range of 3.0–4.0 IPV units, which Hoerling et al. (1991) found to be most realistic for January 1979 from ECMWF data.

Stations are excluded from this comparison if they are within the region of the PJ–trough system where a unique specification of the tropopause from radiosonde reports is often difficult. This exclusion ensures that erroneously reported station tropopause pressures do not affect the choice of an IPV surface to represent the tropopause. Due to the quasi conservation of IPV for

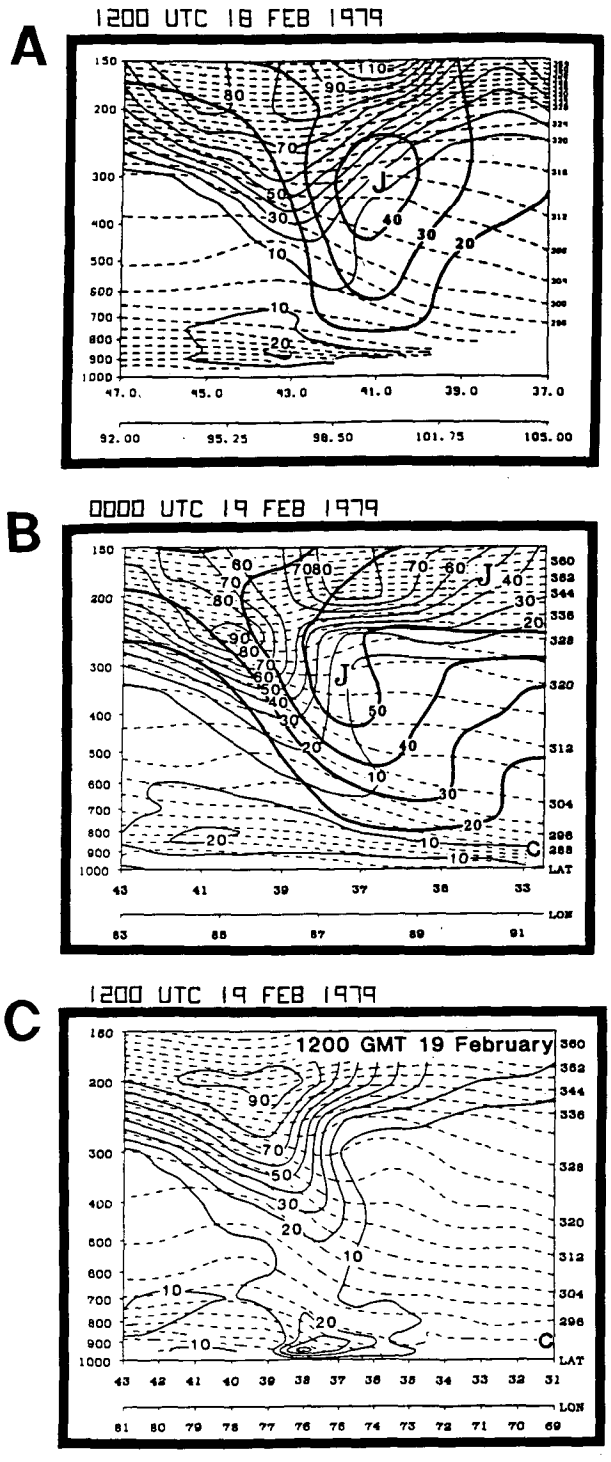

FIG. 3. Cross sections through PJ–trough system at (a) 1200 UTC 18 February, (b) 0000 UTC 19 February, and (c) 1200 UTC 19 February 1979 depicting isentropes (K, dashed), potential vorticity (10^{-6} K mb^{-1} s^{-1}, thin solid), and isotachs [(a) and (b) only; m s^{-1}, heavy solid] (reproduced from Whitaker et al. 1988). Locations are indicated by bold straight lines in Fig. 2. Note that due to differences in the definition of IPV, values in these cross sections are approximately a factor of 10 larger than the IPV used in this study as defined by Eq. (2).

stratospheric air passing from undisturbed regions into the PJ–trough system, the value of IPV found to define the tropopause in the undisturbed regions is then used to represent the tropopause within the PJ–trough system. For example, the soundings for Omaha and Huron at 1200 UTC 18 February, and Peoria and Salem at 0000 UTC 19 February (Fig. 4), lie within the region of the PJ–trough system (see Fig. 2). The reported tropopauses at all stations except Peoria are well above inversion or isothermal layers found between 300 and 400 mb. These layers are associated with the upper-level front depicted in the cross sections (Fig. 3) and therefore likely represent stratospheric air (Danielson 1968).

Additional stations lying within the model domain are excluded from the comparison if, within the vertical profile at the model grid point corresponding to the station location, no tropopause could be found below the 100-mb upper boundary of the MASS model data using a 4.0-IPV-unit criterion. These points are located on the anticyclonic shear side of the subtropical jet (see Fig. 9). Stations excluded from the comparison at 0000 UTC 19 February are marked by the letter "X" in Fig. 6.

The analysis to match reported tropopause and IPV surface pressures is performed using 1) the average difference of station pressures and gridpoint pressures (bold solid line), 2) the average of the absolute value of these differences (dashed line), and 3) the root-mean-square of these differences (thin solid line). These comparisons (Fig. 5) show that the best agreement for the three times always occurs within a range of IPV values between 2.7 and 3.5 IPV units. Based on this analysis, 3.0 IPV units will be used to depict the tropopause.

The station tropopause pressures minus the pressures on the MASS model's 3.0-IPV surface at 0000 UTC 19 February are plotted at the station locations (Fig. 6a). The magnitude and sign of the differences seem to be randomly distributed throughout the model domain with no strong dependence on geographical location. In contrast, the differences on the 1.5-IPV surface (Fig. 6b) are consistently negative with large magnitudes in the southern and eastern portions of the model domain.

At 1200 UTC 18 February, the correspondence between the 3.0-IPV-unit surface determined from the model's initial data field and the upper-level front found in the station soundings (Figs. 4a,b) confirms that this IPV surface is able to identify the upper-level front within the PJ–trough system. The continuing agreement 12 h later between the model-determined 3.0-IPV-unit surface and the location of the upper-level front on the station soundings (Figs. 4c,d) confirms that the upper-level front is being depicted by the model simulation.

The evolution of the pressure distributions on the tropopause surface defined by 3.0 IPV units is shown

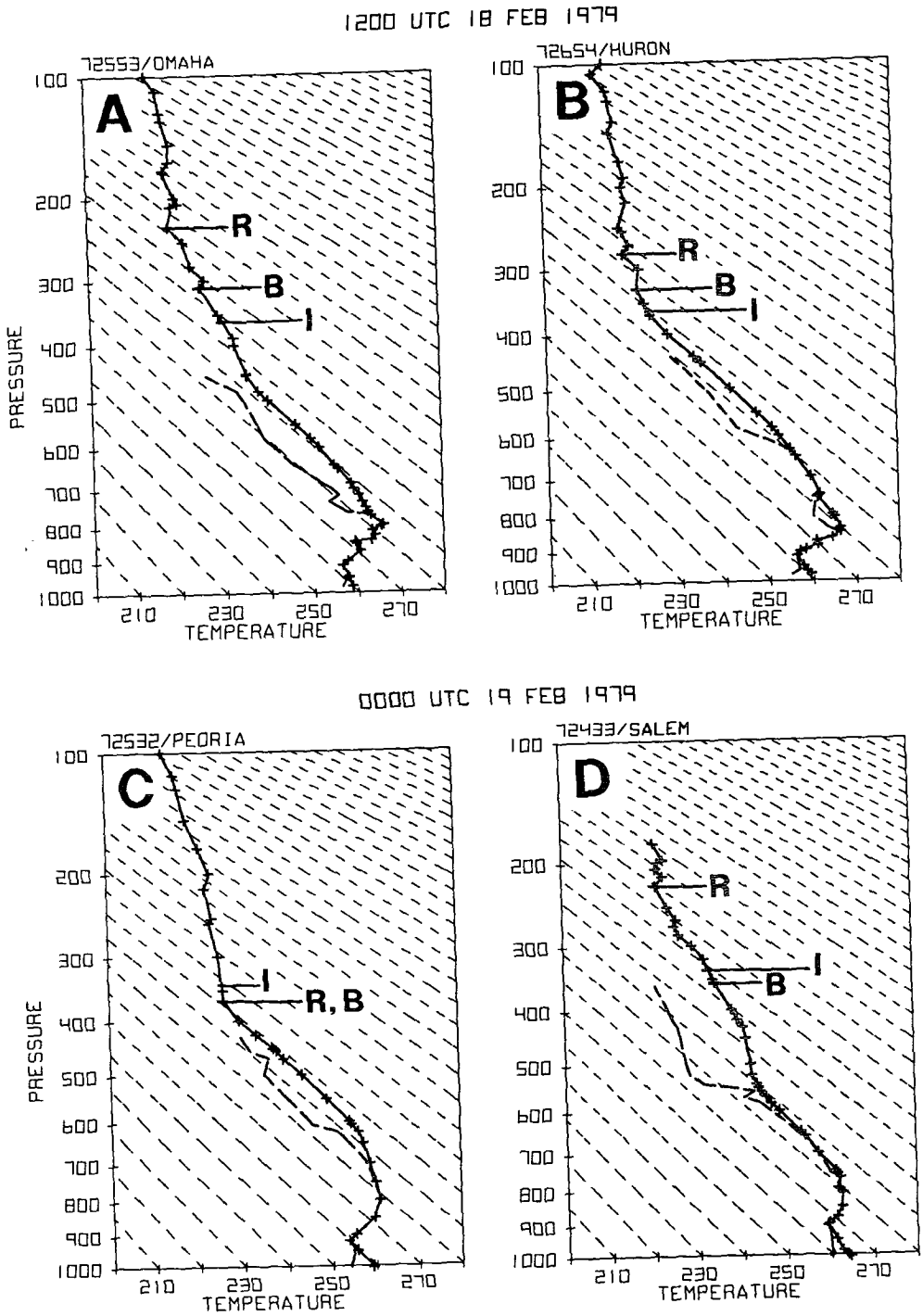

FIG. 4. Soundings for (a) Omaha and (b) Huron at 1200 UTC 18 February, and (c) Peoria and (d) Salem at 0000 UTC 19 February 1979. The station-reported tropopause is denoted by "R," the base of the lowest inversion or nearly isothermal layer above 500 mb is denoted by "B," and the pressure on the 3.0-IPV-unit surface is denoted by "I."

in Fig. 7. A comparison of the highest tropopause pressures on the 3.0-IPV surfaces with the model-predicted troughs on the 312-K surfaces (Fig. 2) reveals that throughout the period of study the tropopause depression accompanies the PJ–trough system. The maximum pressures are consistently located

near the trough axis on the cyclonic side of the strongest winds.

The center of the depressed tropopause moves from southeastern South Dakota southeastward to southern Indiana and then eastward to a position off the Delmarva peninsula. Maximum pressures are generally between 380 and 420 mb. The strongest gradients of pressure on the depressed tropopause rotate from the southwest side to the southeast side in association with the propagation of the baroclinic support for the jet through the trough.

Qualitative evidence of the appropriateness of the IPV surface to define the tropopause can be seen by comparing the pressure distribution on the IPV surface to the total ozone in a vertical column of the atmosphere obtained from the total ozone mapping spectrometer (TOMS). Schubert and Munteanu (1988) have documented a positive correlation between total ozone and tropopause pressure. TOMS observations, which were available at 1802 UTC 18 February and 1637 UTC 19 February, are compared to the pressure distributions on the 3.0-IPV-unit surface for corresponding times (Fig. 8). This comparison demonstrates a close correspondence between maximum ozone concentration and high pressures on an IPV-determined tropopause. These results together with the previously established correlation between the 3.0-IPV-unit surface and observed tropopause pressures suggest that a reasonable definition of the tropopause has now been established to calculate stratospheric–tropospheric exchange.

5. Stratospheric–tropospheric mass exchange

Stratospheric–tropospheric exchange is estimated over a quasi-Lagrangian rectangular domain of approximately 10^{12} m^2 centered on and moving with the maximum pressure on the depressed tropopause. Transport from the stratosphere to the troposphere is estimated by areally integrating over the region of transport across the 3.0-IPV-unit surface from higher to lower values of IPV. Similarly, transport from the troposphere to the stratosphere is estimated by integrating over the region of transport from lower to higher values. The net transport within the domain is simply the sum of these two components.

The calculations, made at 3-h intervals between 1500 UTC 18 February and 1500 UTC 19 February, provide estimates of transport for the period when the tropopause depression is strongly developed and intense surface cyclogenesis is initiated (see Whitaker et al. 1988 for surface analyses). The computational period begins 3 h following the initiation of the simulation to allow time for the model to generate a consistent atmospheric structure. After 1500 UTC 19 February, the approach of the depressed tropopause to the eastern boundary of the model domain precludes reasonable estimates of exchange.

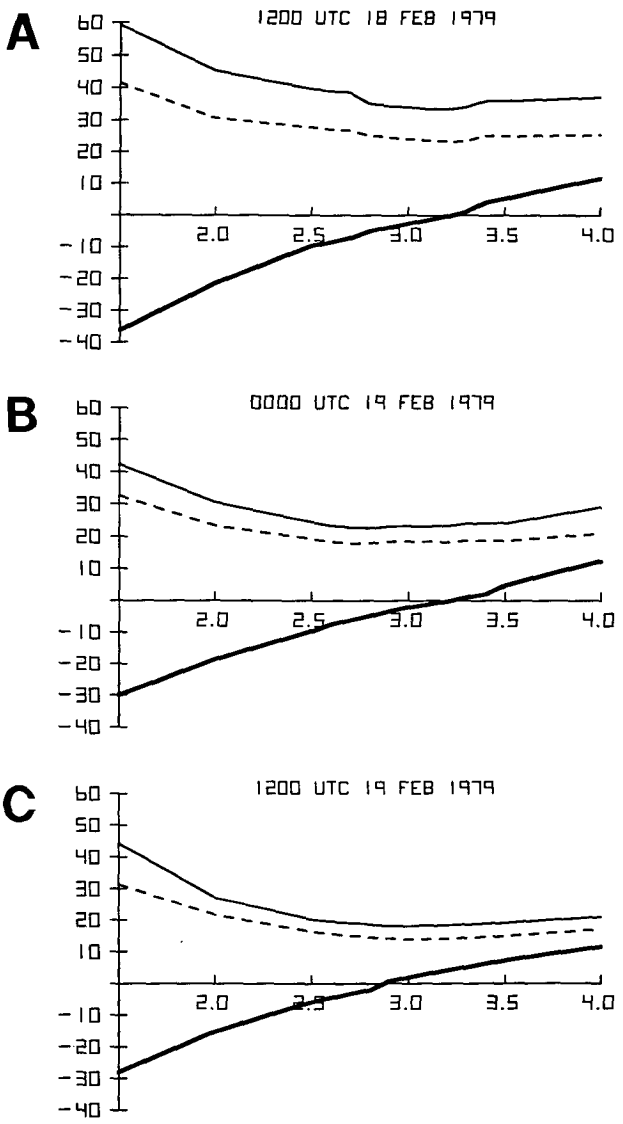

FIG. 5. Graphical representation of differences (mb, y axis) as a function of IPV (x axis) between tropopause pressures reported by radiosonde stations and pressures on IPV surfaces at station locations. The dark solid line is the average difference, the dashed line is the average of the absolute value of the differences, and the light solid line is the root-mean-square of the differences. Graphical representations are for (a) 1200 UTC 18 February, (b) 0000 UTC, and (c) 1200 UTC 19 February 1979.

At 1200 UTC 18 February, local maxima of potential temperature on the IPV tropopause surface were encountered along the northern and western boundaries of the model domain near International Falls, Minnesota, and Denver, Colorado, respectively (see Fig. 9). Another is apparent on the western boundary 3 h later (not shown). These regions of anomalous potential temperature then propagate into the model domain. The magnitudes of these extremes decrease steadily with time, although remnants of these initial potential tem-

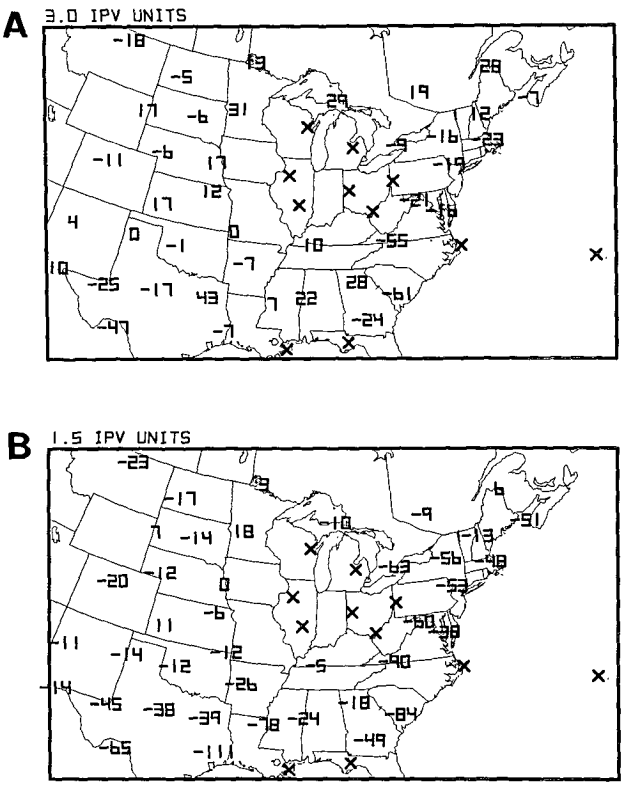

FIG. 6. Horizontal distribution of differences between pressures (mb) reported by radiosonde stations and pressures on the (a) 3.0-IPV-unit surface and (b) 1.5-IPV-unit surface at 0000 UTC 19 February 1979. Radiosonde stations located either within the region of the tropopause depression or at grid points where the 4.0-IPV-unit surface could not be found are indicated by "X."

perature maxima can still be identified near the center of the computational domain until 0600 UTC 19 February. These potential temperature extremes resulted from the incorporation of radiosonde station data into the model from stations located near the model boundary (L. Uccellini 1991, personal communication). The presence of the potential temperature anomalies propagating through the computational domain results in a degradation of the spatial and temporal transport distributions when evaluations are done over the 3-h intervals corresponding to archived model data. However, if the distributions are averaged over 12 or more hours, clear and consistent patterns emerge due to the cancellation with time of the effects of the propagating anomalies. Such cancellation could not be achieved in an Eulerian system.

The stratospheric–tropospheric exchange within the region of strong potential temperature gradients associated with the subtropical jet (see Fig. 9) is not estimated. In this region, the distribution of potential temperature on the tropopause contains several uncertainties. For example, several of the previously mentioned regions of anomalous potential temperature originating along the model's lateral boundaries propagate into the potential temperature gradients associated with the subtropical jet, creating uncertainties in these gradients. Also, an unexplained region of anticyclonic shear exists over Texas at 1200 UTC 18 February, the initial time for the model run (not shown). The region of anticyclonic shear propagates along the subtropical jet, apparent as a distortion in the potential temperature distribution (Fig. 9), reaching the eastern boundary of the model domain on 0300 UTC 19 February. Its presence precludes confident identification of the potential temperature gradient associated with the subtropical jet structure on the 3.0-IPV-unit surface. With the focus of the study being limited to the stratospheric–tropospheric exchange accompanying the PJ–trough system and to retain confidence in the results, the southern boundary of the computational region is located along the poleward edge of the strong potential temperature gradients associated with the subtropical jet. The southern boundary of the computational domain is indicated by the end of the contours in Figs. 10c,d.

The computational domain used in the quasi-Lagrangian analysis lies within a rectangle having lateral boundaries defined by meridians and latitude circles of constant east–west and north–south separation, respectively. The rectangle itself is always centered on and moving with the tropopause depression (see path in Figs. 10a,b). The velocity **W** used in (1) is the velocity of the point of highest pressure on the tropopause depression. The curved path taken by the tropopause depression is reflected in the changing orientation of the vector **W**. The quantities displayed in Fig. 10 are 12-h time averages within the moving computational rectangle superimposed on a base map determined by the average location of the tropopause depression. Specifically, the location of the origin of the axes is determined by the mean latitude and longitude of highest pressure on the tropopause depression during the 12-h period. The axes are used to divide the rectangle into quadrants.

The time-averaged horizontal distributions of stratospheric–tropospheric mass exchange are presented in Figs. 10c,d for each of the 12-h periods (1500 UTC 18 February–0300 UTC 19 February and 0300–1500 UTC 19 February). Two passes of a (2, 3, 2) filter are applied to the 12-h-averaged distributions to provide for clear identification of the features of principal interest. Also shown are the 12-h-averaged tropopause pressures (Figs. 10a,b) and the 12-h-averaged Montgomery streamfunction and isotach analyses (Figs. 10e, f).

During the first 12-h period, transport from the stratosphere to the troposphere (negative values) occurs in the northwest, southwest, and southeast quadrants with largest magnitudes occurring in the northwest quadrant (Fig. 10c). From there, a band of prominent negative values extends to the south of the tropopause depression's time-averaged center. A

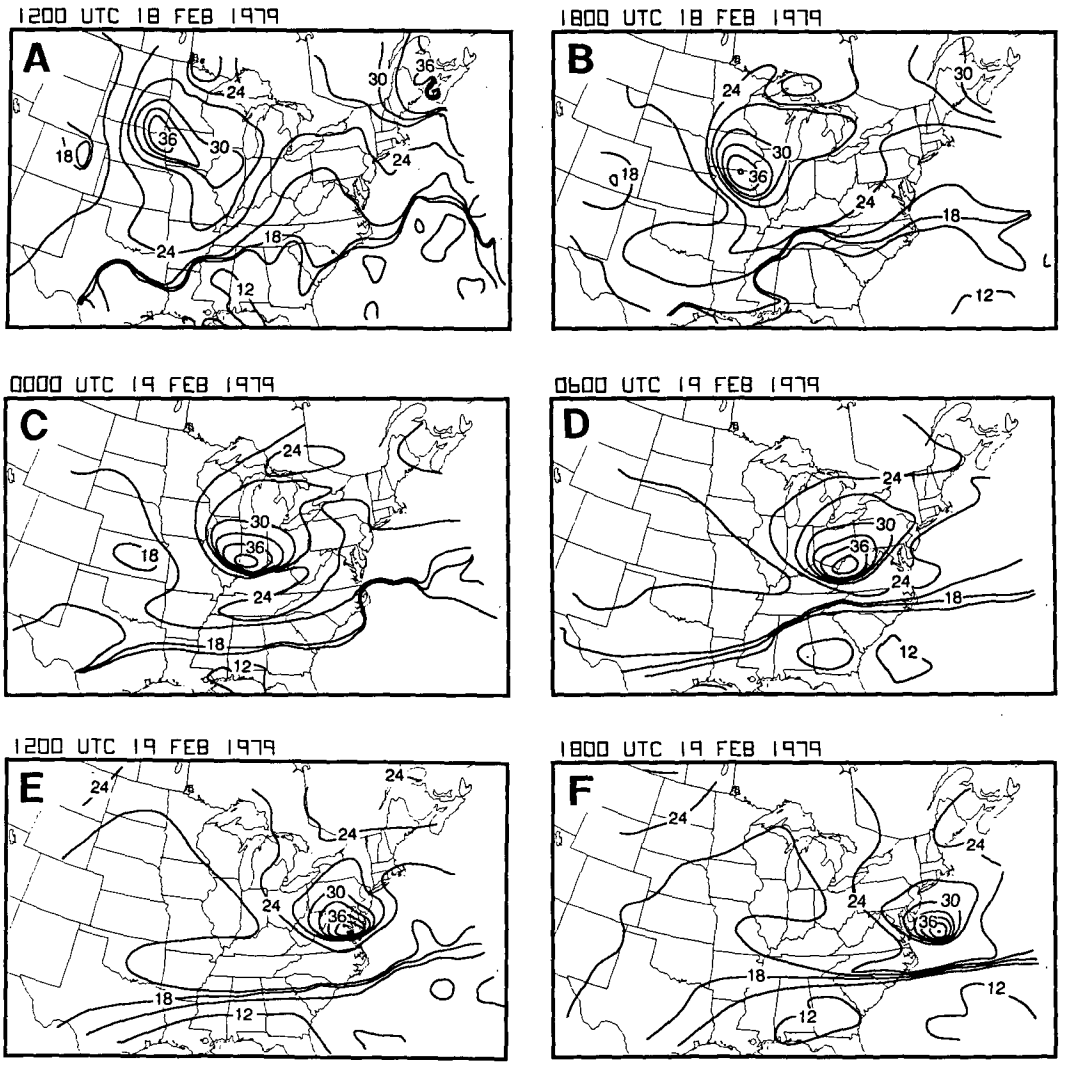

FIG. 7. Distribution of pressure (cb) on the 3.0-IPV-unit surface at 6-h intervals from 1200 UTC 18 February to 1800 UTC 19 February 1979.

smaller area of transport from the troposphere to the stratosphere (positive values) occurs in the northeast quadrant near the center of the tropopause depression.

During the second 12-h period, the general pattern of transport remains the same (Fig. 10d). However, the axis of maximum transport from the stratosphere to the troposphere adopts a more east–west orientation, while largest magnitudes of transport in both directions shift eastward with respect to the time-averaged center of the depressed tropopause. These changes parallel the shift in the strongest pressure gradients on the depressed tropopause. This reflects the shift in the baroclinic support for the polar-front jet stream as it rotates around the trough. This shift is evident in the composite Montgomery streamfunction and isotach distributions on the 312-K isentropic surfaces (Figs. 10e, f).

The horizontal distribution of transport from the stratosphere to the troposphere in each of the two 12-h periods coincides with the descending dry air of stratospheric origin found by Uccellini et al. (1985). Carlson (1980) and Whitaker et al. (1988) refer to this feature as the "dry airstream." The transport from the troposphere to the stratosphere in the northeast quadrant during the second 12-h period agrees with the location of air parcels that have ascended within the "warm and cold conveyer belts" (Carlson 1980). Further, the position is also consistent with the end point of trajectories that originate in lower levels within the warm sector or east of the warm front and subsequently ascend in an anticyclonically curved path (Kuo et al. 1992). Finally, the transport from the troposphere to the stratosphere is consistent with ascending, poleward-moving

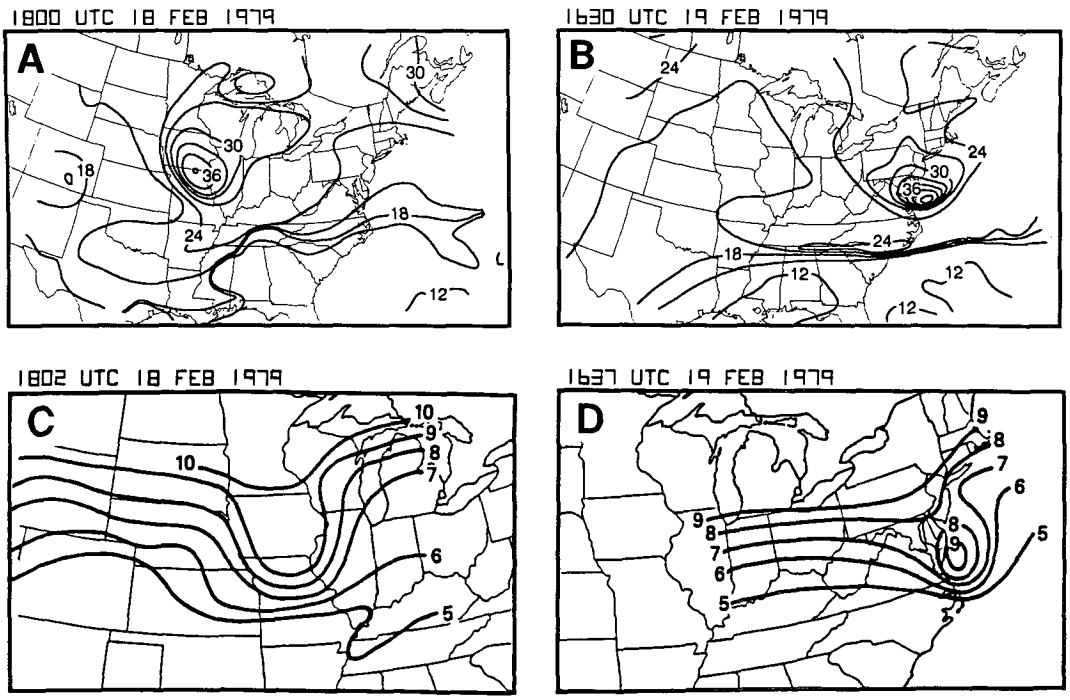

FIG. 8. Comparisons of pressure (cb) on the 3.0-IPV-unit surface to total columnar ozone. Pressures are for (a) 1800 UTC 18 February and (b) 1630 UTC 19 February 1979. Total columnar ozone distributions are for (c) 1802 UTC 18 February and (d) 1637 UTC 19 February 1979 (reproduced from Uccellini et al. 1985). The ozone distribution is in Dobson units (1 DU = 10^{-3} atm cm) with contour intervals as follows: 5–6 (325–339 DU); 6–7 (340–354 DU); etc.

air ahead of a baroclinic wave (Palmén and Newton 1969; Johnson 1979).

Studies of trajectories within storms (e.g., Kuo et al. 1992) show that some trajectories within the dry airstream ascend after passing to the east of the cyclone center. These ascending parcels may contribute to the observed transport from troposphere to stratosphere in Fig. 10. In this case, the assumption that air passing from the stratosphere to the troposphere becomes completely incorporated into the troposphere leads to an overestimate of stratospheric–tropospheric exchange. However, the parcels that reenter the stratosphere would likely have acquired some tropospheric properties through mixing and contribute to transport of these properties into the stratosphere (Shapiro 1980).

Distributions of the three components on the right side of (1) are presented in Fig. 11. The quasi-Lagrangian advective component (Figs. 11e, f) contributes to transport from the stratosphere to the troposphere on the west side of the depression, while a reverse contribution occurs on the east side. Within the eastward-moving quasi-Lagrangian system, the importance of the east–west component of velocity is reduced relative to the north–south component. As a result, the quasi-Lagrangian velocity tends to be directed from lower to higher values of potential temperature on the west side of the tropopause depression and from higher to lower values on the east side, leading to the distributions in Figs. 11e, f . The quasi-Lagrangian tendency of potential temperature contributes to transport from the stratosphere to the troposphere over a large portion of the computational domain (Figs. 11c,d). This results from the decreasing potential temperature with time on the 3.0-IPV surface (see Fig. 3). The contribution to transport from diabatic effects (Figs. 11a,b) is small compared to the contributions from the other two components.

A necessary step to obtain transport estimates using Wei's diagnostic model when the tropopause is represented by an IPV surface is the replacement of a folded IPV surface by a steeply sloping surface on a discrete grid according to the schematic in Fig. 1. The redefined surface is represented as a strong gradient of potential temperature on the discrete grid. There can be uncertainties associated with this computational device. However, the strongest potential temperature gradients, located on the south side of the tropopause depression, are approximately normal to the wind axis. Consequently, the portion of mass transport associated with the advection of potential temperature [third right-hand term of (1)] in the presence of these strong gradients does not overwhelm the total transport $F(\rho)$. This is demonstrated by the time- and area-integrated results discussed herein and shown in Table 2, in which the

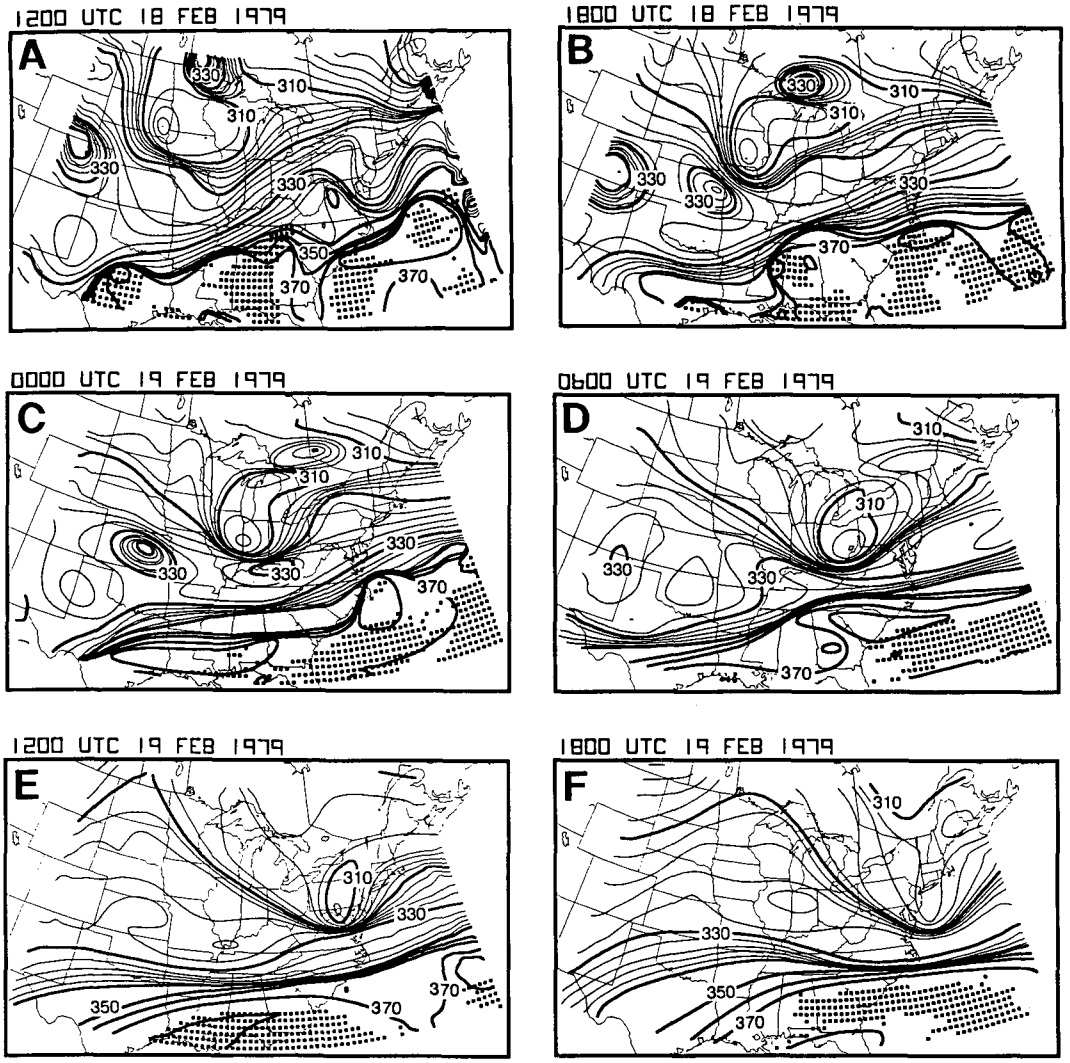

FIG. 9. Distributions of potential temperature on the 3.0-IPV-unit surface at 6-h intervals from 1200 UTC 18 February to 1800 UTC 19 February 1979. Contour interval is 10 K with supplemental contours at 2 K below 340 K. Grid points at which the IPV surface could not be found below 100 mb are identified by a bold dot.

tendency of potential temperature on the right-hand side of (1) is more important than the advection of potential temperature in determining $F(\rho)$. Further, it can be inferred from Figs. 10c,d that the areal distribution of stratospheric–tropospheric exchange is maximized within the region of the tropopause depression rather than being confined to the immediate vicinity of the redefined IPV surface, the latter lying within the strong potential temperature gradients in Fig. 9.

Estimates of the time- and area-integrated transport for the two consecutive 12-h periods beginning at 1500 UTC 18 February, and for the entire 24-h period, are presented in Table 1. The 12-h transport estimates are obtained by first temporally integrating the four 3-h transports at each grid point within the computational rectangle. Grid points are then deleted from the computational domain in the southeast where the effects of the subtropical jet as simulated by the MASS model preclude obtaining confident transport estimates. Finally, an area integration is performed over the remaining grid points. The transports are obtained from the unfiltered form of the horizontal distributions in Figs. 10c,d. The computational area corresponds to the contoured portions of Figs. 10c,d.

The mass transports from the stratosphere to the troposphere are 3×10^{14} kg in the first 12-h period and 2×10^{14} kg in the second, while 1×10^{14} kg pass from the troposphere to the stratosphere in each of the 12-h periods. The net 12-h transports are from the stratosphere to the troposphere with magnitudes of 2×10^{14} and 1×10^{14} kg, respectively. Twenty-four-hour transport estimates, based on the sum of the two 12-h estimates, have

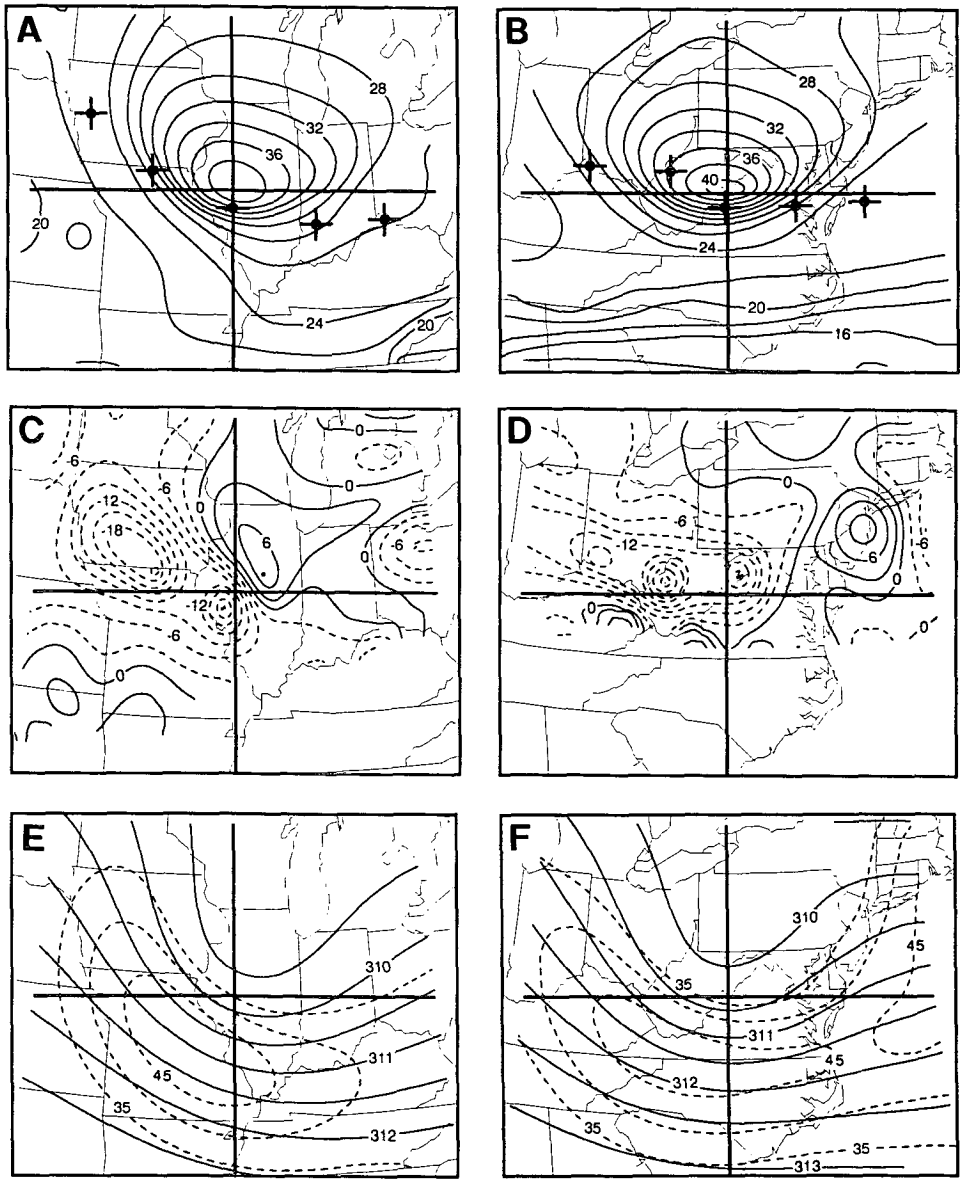

FIG. 10. Distributions averaged over 12 h within the moving coordinate system of pressure (cb) [(a) and (b)] and mass transport (10^{-3} kg m^{-2} s^{-1}) [(c) and (d)] on the 3.0-IPV-unit surface, and 312-K Montgomery streamfunction (10^3 m^2 s^{-2}) and isotachs (m s^{-1}) [(e) and (f)]. Panels (a), (c), and (e) are for 1500 UTC 18 February–0300 UTC 19 February; (b), (d), and (f) are for 0300–1500 UTC 19 February. Isotachs less than 35 m s^{-1} are not shown. Horizontal and vertical bold lines intersect average position of highest pressure on IPV surface during the 12-h period. The 3-h positions of highest pressure are denoted by crosses in panels (a) and (b). Negative values in (c) and (d) indicate transport from stratosphere to troposphere.

5×10^{14} kg passing from the stratosphere to the troposphere and 2×10^{14} kg passing from the troposphere to the stratosphere, leaving a net transport of 3×10^{14} kg passing from the stratosphere to the troposphere.

The transport from the stratosphere to the troposphere during the 24-h period is very close to the estimate of 6×10^{14} kg found by Reiter and Mahlman (1965) for "a case of cyclogenesis of average intensity and radioactive fallout over North America from November 22 to 23, 1962" (Reiter 1975). The transport from the stratosphere to the troposphere during the 24-h period is 2.5 times larger than the transport from the troposphere to the stratosphere. This agrees with the 2:1 ratio suggested by Reiter et al. (1969), who estimated exchange from motion along isentropic surfaces intersecting the tropopause.

During the 24-h period, the net transport of approximately 3×10^{14} kg is from the stratosphere to the

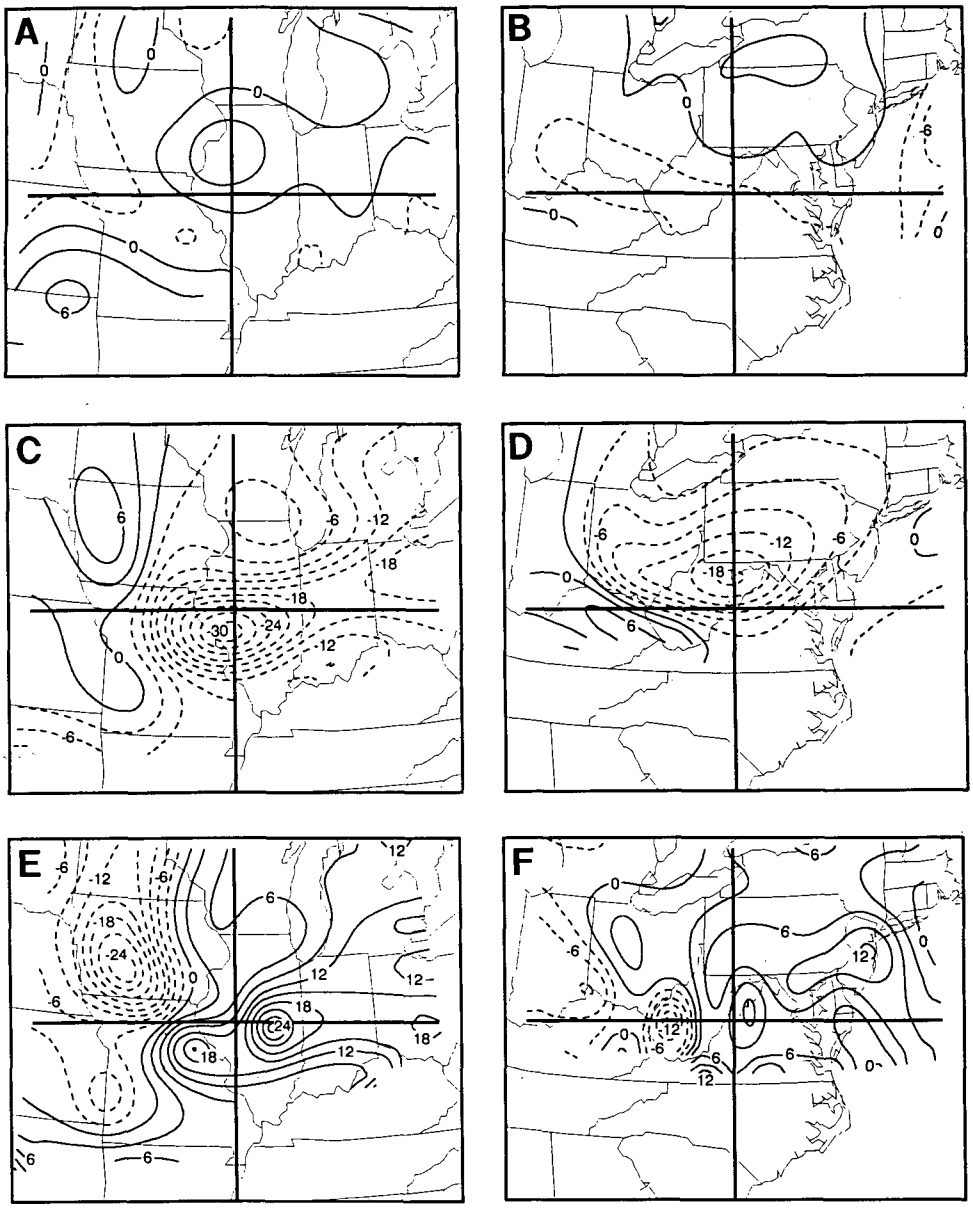

FIG. 11. Distributions averaged over 12 h within the moving coordinate system of contributions to mass transport (10^{-3} kg m^{-2} s^{-1}) across the 3.0-IPV-unit surface from diabatic processes [(a) and (b)] and from the quasi-Lagrangian tendency [(c) and (d)] and advection [(e) and (f)] of potential temperature. Panels (a), (c), and (e) are for 1500 UTC 18 February–0300 UTC 19 February; (b), (d), and (f) are for 0300–1500 UTC 19 February. Horizontal and vertical bold lines intersect the average position of highest pressure on IPV surface during the 12-h period. Negative values indicate transport from stratosphere to troposphere.

troposphere. Hoerling et al. (1993) estimated a transport of 64×10^{15} kg from the stratosphere to the troposphere between 25° and 50°N during a 29-day period in January 1979. This is approximately an average daily transport of 2×10^{15} kg. Therefore, during a 24-h period, a system such as the Presidents' Day storm is capable of providing about one-seventh of the average daily exchange estimated for a winter month within this latitude band.

The time- and area-integrated contributions of the components on the right side of (1) to the total transport are shown in Table 2. Diabatic effects are not significant in the time- and area-integrated results. The quasi-Lagrangian tendency of potential temperature makes the largest contribution and is associated with transport from the stratosphere to the troposphere. Fifty percent of this contribution is offset by the advective component.

TABLE 1. Stratospheric–tropospheric mass exchange (10^{14} kg) based on transport across the 3.0-IPV-unit surface. Negative values denote transport from stratosphere to troposphere. Corresponding results from the University of Wisconsin $\theta-\sigma$ model are in parentheses.

Time period	Net transport	Stratosphere to troposphere	Troposphere to stratosphere
1500 UTC 18 February–0300 UTC 19 February 1979	−2 (−2)	−3 (−3)	1 (1)
0300–1500 UTC 19 February 1979	−1 (−1)	−2 (−3)	1 (2)
1500 UTC 18 February–1500 UTC 19 February 1979	−3 (−3)	−5 (−6)	2 (3)

To assess the sensitivity of transport estimates to a particular model's ability to simulate the atmosphere, transport estimates are presented from a second independent model simulation of the Presidents' Day storm. This simulation was conducted using the regional University of Wisconsin (UW) hybrid $\theta-\sigma$ model (Zapotocny et al. 1993). Above a σ domain 150 mb thick, this model uses potential temperature θ as the vertical coordinate, while the MASS model uses σ throughout. Since the tropopause is, by definition (see section 2), at least 150 mb above the earth's surface, potential temperature is effectively the model vertical coordinate from which the tropopause and stratospheric–tropospheric exchange are determined.

The UW $\theta-\sigma$ model uses physical parameterizations of surface sensible heating, evaporational sources of water vapor at the earth–atmosphere interface; skin friction; dry convective adjustment; ground wetness; surface snow, ice and frost cover; vertical diffusion of heat and moisture; cumulus convection; and moist-adiabatic adjustment. Additionally, large-scale interactive clouds and the National Center for Atmospheric Research Community Climate Model (CCM1) radiation algorithm have been incorporated.

The time- and area-integrated transport results based on the UW $\theta-\sigma$ model are included in Table 1 (values are in parentheses). These results are based on transport through the 3.0-IPV-unit surface for a quasi-Lagrangian computational region having the same shape, size, and placement with respect to the tropopause depression as used for the MASS model. The transport estimates are clearly consistent with those obtained using the MASS model. During the first 12 h, there is no difference to one significant digit. During the second 12 h, the UW $\theta-\sigma$ model's transport across the troposphere is one unit larger in both directions with the result that the net transport is the same as the MASS model. Additionally, the spatial distributions of transport with respect to the tropopause depression using the UW $\theta-\sigma$ model simulation (not shown) are consistent with those shown in Figs. 10c,d from the MASS model simulation. The results from the UW $\theta-\sigma$ model simulation provide both qualitative and quantitative corroboration for the transport estimates obtained using the MASS model simulation.

6. Summary

The exchange of mass between the stratosphere and troposphere was studied for a case of intense cyclogenesis using results from the MASS numerical model simulation of the Presidents' Day storm of 18–19 February 1979 (Whitaker et al. 1988). The initial part of the study consisted of determining an appropriate value of IPV to represent the tropopause. A comparison of tropopause pressures reported by radiosonde stations to the pressures on various IPV surfaces between 1.5 and 4.0 IPV units demonstrated that the 3.0-IPV-unit surface provided a good estimate of the tropopause. This value, although larger than the 1.6-IPV-unit World Meteorological Organization criterion (World Meteorological Organization 1986), is consistent with the 3.0–4.0-IPV-unit range of optimum values found by Hoerling et al. (1991).

Mass transport across the 3.0-IPV surface was calculated using the diagnostic transport model of Wei (1987) applied within a quasi-Lagrangian reference system. The size of the quasi-Lagrangian region was approximately 10^{12} m^2. Three-hourly transports in the moving reference system were calculated and integrated over each of two consecutive 12-h periods spanning an interval when the tropopause depression was

TABLE 2. Contribution to stratospheric–tropospheric mass exchange (10^{14} kg) from diabatic processes and the quasi-Lagrangian advection and tendency of potential temperature. Negative values denote transport from the stratosphere to the troposphere.

Time period	Component contributions		
	$\rho J_\theta(\mathbf{U}-\mathbf{W})\cdot\nabla_Q\theta$	$\rho J_\theta \delta\theta/\delta t_Q$	$\rho J_\theta \dot{\theta}$
1500 UTC 18 February–0300 UTC 19 February 1979	2	−4	0
0300–1500 UTC 19 February 1979	1	−2	0
1500 UTC 18 February–1500 UTC 19 February 1979	3	−6	0

strongly developed and explosive surface cyclogenesis commenced. During the entire 24-h period, 5×10^{14} kg passed from the stratosphere to the troposphere, while 2×10^{14} kg passed from the troposphere to the stratosphere. The 5:2 ratio of these two transports is consistent with the 2:1 ratio suggested by Reiter et al. (1969). Additionally, the value of transport from the stratosphere to the troposphere agrees well with the estimate of Reiter and Mahlman (1965) during "a case of cyclogenesis of average intensity."

The net transport over the 24-h period was 3×10^{14} kg from the stratosphere to the troposphere. Based on the Hoerling et al. (1993) estimate of 64×10^{15} kg of mass transport from the stratosphere to the troposphere between 25° and 50°N for January 1979, a system such as the Presidents' Day storm is capable of providing approximately one-seventh of the average daily net cross-tropopause transport within this latitude band for a winter month.

Transport from the stratosphere to the troposphere occurred in an arc extending from northwest through east around the PJ–trough system. This coincides with the analysis by Uccellini et al. (1985) of descending stratospheric air, which has been referred to as the dry airstream (Carlson 1980; Whitaker et al. 1988). The reverse transport from the troposphere to the stratosphere in the northeast quadrant during the second 12-h period is consistent with ascending trajectories analyzed by Carlson (1980) and Kuo et al. (1992). The transport is also consistent with ascending, poleward-moving air ahead of a baroclinic wave (Palmén and Newton 1969; Johnson 1979).

The present study demonstrates that estimates of stratospheric–tropospheric mass exchange using Wei's transport equation in a quasi-Lagrangian reference system are reasonable. The results agree with independent transport estimates (Reiter and Mahlman 1965; Reiter et al. 1969) and are consistent with models of airstreams within extratropical cyclones (Carlson 1980). Finally, similar results were obtained from both the MASS model simulation of the Presidents' Day storm (Whitaker et al. 1988) and a second, independent simulation using the regional University of Wisconsin hybrid $\theta-\sigma$ model (Zapotocny et al. 1993).

The results presented here, however, should be regarded only as preliminary. They are subject to uncertainties including the redefinition of IPV surfaces in the presence of tropopause folds, the assumption that air crossing the 3.0-IPV-unit surface is entirely incorporated into the portion of the atmosphere it enters, and the ability of the models to simulate the real atmosphere. A more definitive statement on stratospheric–tropospheric exchange requires further research using Wei's diagnostic model to study different types of midlatitude systems, with a variety of observed and model-generated datasets. Additionally, evaluating transport as a function of IPV should be done. By examining the correlation of transport through the IPV surface defining the tropopause with the transports through surfaces having lower and higher values of IPV, the question of how thoroughly mass is incorporated into the region of the atmosphere it enters after passing through the tropopause can be addressed. Finally, trajectory analysis should be performed. Such an analysis would provide verification of the distribution of exchange.

Acknowledgments. This study was in part motivated by the previous work of Drs. Ming-Ying Wei and Martin Hoerling. The University of Wisconsin hybrid $\theta-\sigma$ model data and helpful comments were provided by Dr. Tom Zapotocny. Preparation of the data used to compute the results in this study was done by Dr. Allen Lenzen. The MASS model simulation was obtained from the Goddard Laboratory for Atmospheres through Dr. Louis Uccellini. The paper benefited substantially from the suggestions of Dr. Frederick Sanders and the anonymous reviewers. Tonya Ommodt assisted in the preparation of the figures. This research was supported by the National Aeronautics and Space Administration under NASA Grant NAG5-81.

REFERENCES

Atlas, R., 1987: The role of oceanic fluxes and initial data in the numerical prediction of an intense coastal storm. *Dyn. Atmos. Oceans,* **10,** 359–388.

Bosart, L. F., 1981: The Presidents' Day snowstorm of 18–19 February 1979: A subsynoptic-scale event. *Mon. Wea. Rev.,* **109,** 1542–1566.

——, and S. C. Lin, 1984: A diagnostic analysis of the Presidents' Day storm of February 1979. *Mon. Wea. Rev.,* **112,** 2148–2177.

Carlson, T. N., 1980: Airflow through midlatitude cyclones and the comma cloud pattern. *Mon. Wea. Rev.,* **108,** 1498–1509.

Danielsen, E. F., 1968: Stratospheric–tropospheric exchange based on radioactivity, ozone and potential vorticity. *J. Atmos. Sci.,* **25,** 502–518.

——, and R. S. Hipskind, 1980: Stratospheric–tropospheric exchange at polar latitudes in summer. *J. Geophys. Res.,* **85,** 393–400.

Hoerling, M. P., T. K. Schaack, and A. J. Lenzen, 1991: Global objective tropopause analysis. *Mon. Wea. Rev.,* **119,** 1816–1831.

——, ——, and ——, 1993: A global analysis of stratospheric–tropospheric exchange during northern winter. *Mon. Wea. Rev.,* **121,** 162–172.

Johnson, D. R., 1977: Generalized transport relations for parametric grid volumes. Isentropic numerical models: Results on model development for zonally averaged and secondary circulations. Report to NSF, Department of Meteorology and Space Science and Engineering Center, University of Wisconsin, Madison, 279–293. [NTIS PB283480/AS.]

——, 1979: Systematic stratospheric–tropospheric exchange through quasi-horizontal transport processes within active baroclinic waves. *WMO Symp. on the Long-Range Transport of Pollutants and Its Relation to General Circulation Including Stratospheric/Tropospheric Exchange Processes,* Sofia, Bulgaria, World Meteorological Organization, 401–408.

——, and W. K. Downey, 1975: Azimuthally averaged transport and budget equations for storms: Quasi-Lagrangian diagnostics 1. *Mon. Wea. Rev.,* **103,** 967–979.

Kuo, Y.-H., R. J. Reed, and S. Low-Nam, 1992: Thermal structure and airflow in a model simulation of an occluded marine cyclone. *Mon. Wea. Rev.,* **120,** 2280–2297.

Palmén, E., and C. W. Newton, 1969: *Atmospheric Circulation Systems: Their Structure and Physical Interpretation.* Academic Press, 603 pp.

Reed, R. J., 1955: A study of a characteristic type of upper-level frontogenesis. *J. Meteor.*, **12,** 226–237.

Reiter, E. R., 1975: Stratospheric–tropospheric exchange processes. *Rev. Geophys. Space Phys.*, **13,** 459–474.

——, and J. D. Mahlman, 1965: Heavy radioactive fallout over the southern United States, November 1962. *J. Geophys. Res.*, **70**(18), 4501–4520.

——, M. E. Glasser, and J. D. Mahlman, 1969: The role of the tropopause in stratospheric–tropospheric exchange processes. *Pure Appl. Geophys.*, **12,** 185–218.

Schaack, T. K., D. R. Johnson, and M.-Y. Wei, 1990: The three-dimensional distribution of atmospheric heating during the GWE. *Tellus,* **42A,** 305–327.

Schubert, S. D., and M. Munteanu, 1988: An analysis of tropopause pressure and total ozone correlations. *Mon. Wea. Rev.*, **116,** 569–582.

Shapiro, M. A., 1980: Turbulent mixing within tropopause folds as a mechanism for the exchange of chemical constituents between the stratosphere and troposphere. *J. Atmos. Sci.*, **37,** 994–1004.

Staley, D. O., 1962: On the mechanism of mass and radioactivity transport from stratosphere to troposphere. *J. Atmos. Sci.*, **19,** 450–467.

Uccellini, L. W., P. J. Kocin, R. A. Petersen, C. H. Wash, and K. F. Brill, 1984: The Presidents' Day cyclone of 18–19 February 1979: Synoptic overview and analysis of the subtropical jet streak influencing the precyclogenetic period. *Mon. Wea. Rev.*, **112,** 31–55.

——, D. Keyser, K. F. Brill, and C. H. Wash, 1985: The Presidents' Day cyclone of 18–19 February 1979: Influence of upstream trough amplification and associated tropopause folding on rapid cyclogenesis. *Mon. Wea. Rev.*, **113,** 962–988.

Uccellini, L. W., R. A. Petersen, K. F. Brill, P. J. Kocin, and J. J. Tuccillo, 1987: Synergistic interactions between an upper-level jet streak and diabatic processes that influence the development of a low-level jet and a secondary coastal cyclone. *Mon. Wea. Rev.*, **115,** 2227–2261.

Wei, M.-Y., 1987: A new formulation of the exchange of mass and trace constituents between the stratosphere and troposphere. *J. Atmos. Sci.*, **44,** 3079–3086.

Whitaker, J. S., L. W. Uccellini, and K. F. Brill, 1988: A model-based diagnostic study of the rapid development phase of the Presidents' Day cyclone. *Mon. Wea. Rev.*, **116,** 2337–2365.

World Meteorological Organization, 1986: Atmospheric ozone 1985: Global ozone research and monitoring report. Report No. 16, WMO, 392 pp.

Zapotocny, T. H., D. R. Johnson, and F. M. Reames, 1993: A comparison of regional isentropic–sigma and sigma model simulations of the January 1979 Chicago blizzard. *Mon. Wea. Rev.*, **121,** 2115–2135.